Geological Society of America Bulletin

Evaluation of $\delta^{13}C$ chemostratigraphy for intrabasinal correlation: Vendian strata of northeast Siberia

Shane M. Pelechaty, Alan J. Kaufman and John P. Grotzinger

Geological Society of America Bulletin 1996;108;992-1003
doi: 10.1130/0016-7606(1996)108<0992:EOCCFI>2.3.CO;2

Evaluation of $\delta^{13}C$ chemostratigraphy for intrabasinal correlation: Vendian strata of northeast Siberia

Shane M. Pelechaty *Department of Earth, Atmospheric and Planetary Sciences, Massachusetts Institute of Technology, Cambridge, Massachusetts 02139*

Alan J. Kaufman *Botanical Museum, Harvard University, Cambridge, Massachusetts 02138*

John P. Grotzinger *Department of Earth, Atmospheric and Planetary Sciences, Massachusetts Institute of Technology, Cambridge, Massachusetts 02139*

ABSTRACT

Integrated sedimentologic, stratigraphic, and geochemical ($\delta^{13}C$, $\delta^{18}O$, Fe, Mn, and Sr) data from Vendian–Cambrian carbonate-ramp deposits of the northeast Siberian platform (Olenek uplift and Kharaulakh Mountains region) are used to constrain primary, time-dependent oscillations in the carbon isotope record and to evaluate $\delta^{13}C$ chemostratigraphy for high-resolution intrabasinal correlation. The Vendian $\delta^{13}C$ record of northeast Siberia reflects global variations seen elsewhere by displaying (in ascending order) a strong positive isotopic shift to values near +6‰ (herein named the P-interval), an intermediate interval of relatively little isotopic change (I-interval), which shows, in some sections, a monotonic decrease in $\delta^{13}C$ from +2‰ at the base to near 0‰ at the top, and a negative excursion to ≈–4‰ (N-interval) just beneath the Vendian-Cambrian boundary. In addition to secular isotopic shifts, these strata exhibit local small-scale signals related to intrabasinal variations in subsidence, erosion, and diagenetic alteration (e.g., degradation of organic matter, dolomitization, and hydrothermal and burial effects). These local, intrabasinal processes, in some cases, have modified both the magnitude and form of the primary isotopic excursions, which are used as the basis for correlation in all studies. Carbon isotope profiles provide an important method to evaluate intrabasinal variations in subsidence, erosion, and stratigraphic completeness. These profiles reflect increasing subsidence along the platform-to-basin transition, whereas progressive truncation of isotopic profiles along this trend illustrate pronounced uplift and erosion of ramp strata along unconformity surfaces.

INTRODUCTION

An emerging $\delta^{13}C$ record of secular variation for Vendian strata is providing an important tool for temporal correlation of rocks that contain only a limited assemblage of flora and fauna necessary for high-resolution chronostratigraphy (Knoll and Walter, 1992). Many workers have identified comparable $\delta^{13}C$ profiles (i.e., $\delta^{13}C$ variations displayed with respect to stratigraphic thickness) from Vendian (ca. 610–543 Ma; Harland et al., 1989; Bowring et al., 1993; Grotzinger et al., 1995) sections around the world (summarized in Ripperdan, 1994; Kaufman and Knoll, 1995), including northwestern Canada (Narbonne et al., 1994), southern China and Morocco (Lambert et al., 1987; Kirschvink et al., 1991; Magaritz et al., 1991), Namibia (Kaufman et al., 1991), Australia (Walter et al., 1995), and Siberia (Magaritz et al., 1986; Pokrovsky and Venagradov, 1991; Kirschvink et al., 1991; Magaritz et al., 1991; Brasier et al., 1993, 1994; Pokrovsky and Missarzhevsky, 1993; Knoll et al., 1995a, 1995b; Pelechaty and Grotzinger, 1993; Pelechaty et al., 1995). This work has formed the basis for the recognition of large-scale secular variations in paleoceanic $\delta^{13}C$ preserved in Vendian carbonates and organic carbon. An oscillating carbon isotope record characterizes Vendian strata overlying diamictites deposited during the latest Proterozoic glaciation (Knoll and Walter, 1992). A prominent negative excursion is noted in carbonate rocks immediately above the diamictites. This negative excusion leads into a positive excursion with $\delta^{13}C$ values as high as +6‰. Then there is an interval of relatively invariant $\delta^{13}C$ values near 0‰. The relatively invariant interval culminates in a distinctive shift to negative values. The $\delta^{13}C$ values return to 0‰ near the Precambrian-Cambrian boundary (Knoll and Walter, 1992; Brasier et al., 1993; Kaufman and Knoll, 1995). The stratigraphic sections used to develop the Vendian chemostratigraphic framework are from isolated sedimentary basins that record a variety of tectonic, depositional, and diagenetic processes. It is important to note that similar large-scale $\delta^{13}C$ variations have emerged despite this geologic diversity.

High-resolution, intrabasinal correlation of Vendian strata using $\delta^{13}C$ chemostratigraphy to assess the influence of depositional and diagenetic processes on the $\delta^{13}C$ isotopic record has not yet been attempted. These processes are known to have diverse effects on primary $\delta^{13}C$ compositions of carbonate (Allen and Matthews, 1982; Arthur et al., 1983; Schidlowski et al., 1984). Diagenetic and stratigraphic studies are necessary to resolve the origin of small-scale variations in carbon isotope values in order to utilize this chronostratigraphic tool for intrabasinal correlations.

The profiles used for correlation are isotopic records that appear continuous in rock thickness, but they are not continuous in time because of depositional hiatuses resulting from unsteady sediment accumulation inherent to stratigraphic sections (Sadler, 1981). The relative completeness of isotopic profiles, however, can be assessed by comparing many profiles from different depositional settings across a single sedimentary basin (Anders et al., 1987; Sadler, 1987). Such a study provides a method

Data Repository item 9642 contains additional material related to this article.

GSA Bulletin; August 1996; v. 108; no. 8; p. 992–1003; 6 figures; 2 tables.

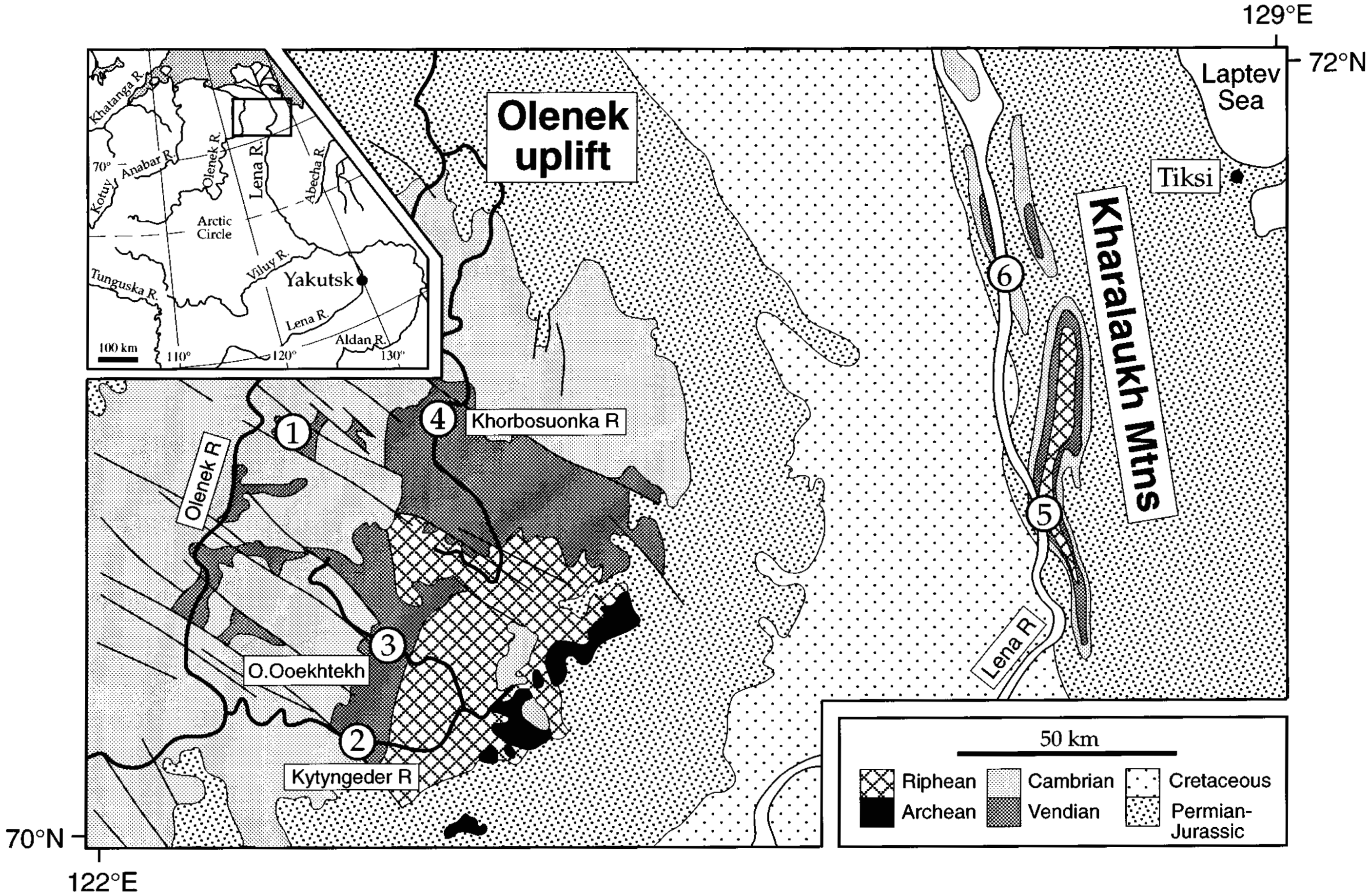

Figure 1. Geologic map of the Olenek uplift and Kharaulakh Mountains region, northeast part of the Siberia platform, Russia. The inset shows the regional geographic setting. Section locations in the Olenek uplift: 1—Olenek River, 2—Kytyngeder River, 3—Oolahan Ooekhtekh River, and 4—Khorbosuonka River. Section locations in the Kharaulakh Mountains: 5—Chekurov anticline and 6—Bokursky anticline.

to examine relative variations in sediment-accumulation rate, which may serve as a proxy for basin subsidence.

This paper presents a detailed geochemical study of several carbonate-dominated stratigraphic sections from the same sedimentary basin. The basin is exposed in the Olenek uplift and Kharaulakh Mountains area of the northeastern corner of the Siberian platform, Russia (Fig. 1). Geochemical data (i.e., $\delta^{13}C$, $\delta^{18}O$, Fe, Mn, and Sr) are presented within a sedimentologic and stratigraphic context in order to assess secular and local signals in the $\delta^{13}C$ composition of the carbonate sediments. In addition to globally recognized, first-order $\delta^{13}C$ shifts, smaller-scale variations are also recognized; these are evaluated in conjunction with stratigraphic and sedimentologic data for use in high-resolution, intrabasinal correlations.

The $\delta^{13}C$ profiles are constructed from stratigraphically closely spaced carbonate samples of minimally altered depositional components. The role of diagenesis in altering the $\delta^{13}C$ composition is assessed by carrying out both component and whole-rock sampling to determine intrasample $\delta^{13}C$ heterogeneity. Standard petrographic, cathodoluminescent, and geochemical proxies are used to determine alteration of carbonate. This work forms the foundation for an integrated basin analysis study using carbon isotope chemostratigraphy and sequence stratigraphy (Pelechaty et al., 1995, 1996).

GEOLOGIC SETTING: STRATIGRAPHY AND DEPOSITIONAL FACIES

Stratigraphy

Vendian carbonate rocks are exposed along several river valleys in the Olenek uplift and along the Lena River 100 km to the east in the Kharaulakh Mountains in the northeastern part of the Siberian platform (Fig. 1). The carbonates consist of both limestone and dolostone. From the Olenek uplift, these strata dip gently outward in all directions and are offset by small-scale (tens of metres of displacement), steeply dipping normal faults (Krasilshchikov and Biterman, 1970). In the Kharaulakh Mountains, the Vendian carbonate strata are deformed into west-verging folds of the post-Cretaceous Verkoyansk fold-and-thrust belt (Rodgers, 1991).

Vendian strata are <500 m thick and are bounded by regional unconformities. The Riphean-Vendian boundary is an angular unconformity that cuts down deepest into Riphean strata of the southern Olenek uplift. The Vendian-Cambrian boundary is a paleokarst erosion surface overlain by Lower Cambrian (Nemakit-Daldyn Stage) siliciclastic and minor limestone strata and rare volcanic deposits (Repina et al., 1974; Valkov, 1987; Khomentovsky and Karlova, 1993; Bowring et al., 1993; Knoll et al., 1995a). These strata thin eastward toward the Kharaulakh Mountains and are everywhere overlain by distinctively red, hyolithid-bearing Tommotian limestone.

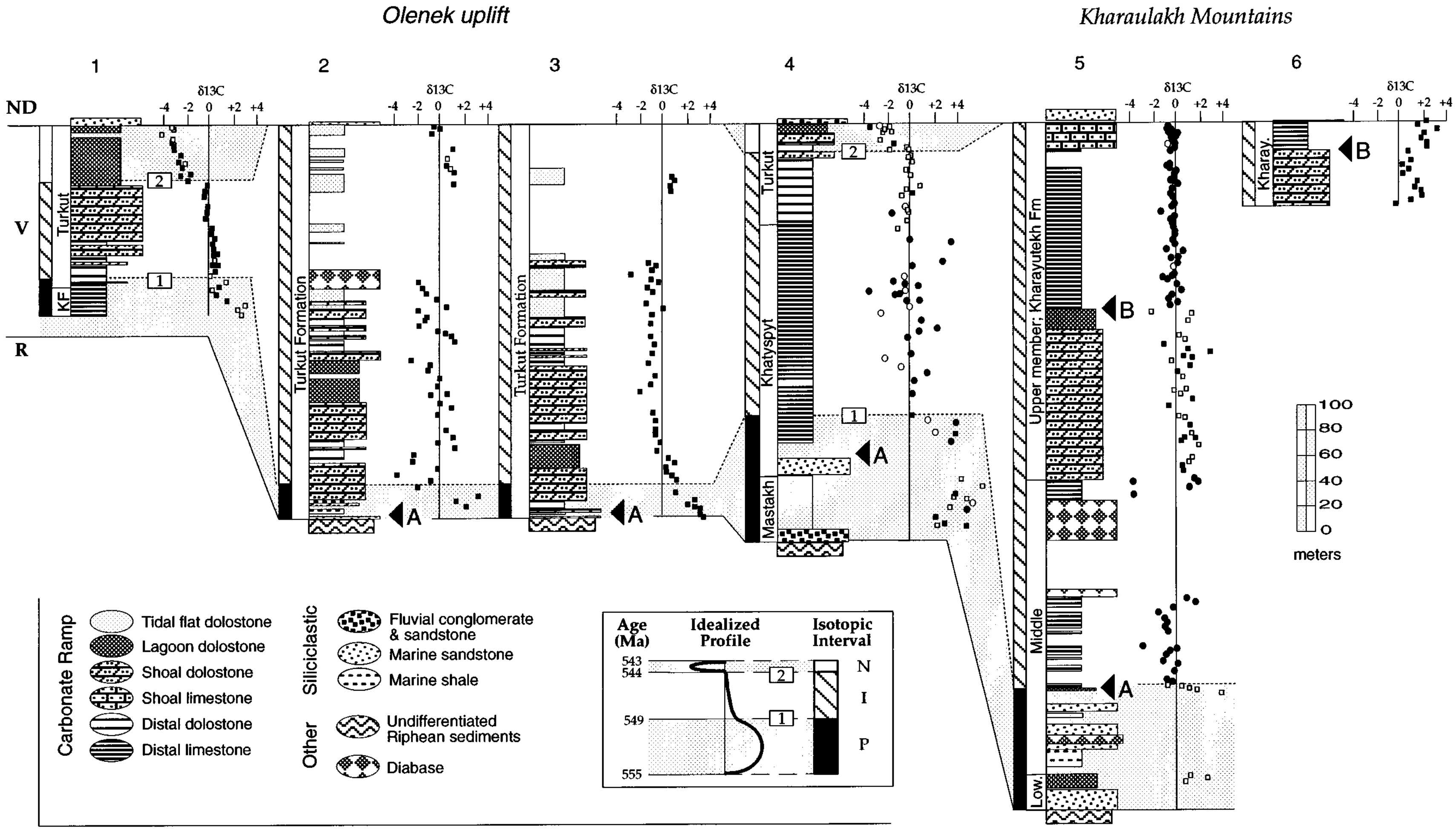

Figure 2. Chemostratigraphic cross section showing stratigraphic sections and their associated $\delta^{13}C$ profiles. The section 4 data are from Knoll et al. (1995a). The sections (refer to Fig. 1 for locations) are hung from a paleokarst unconformity present at the top of all sections. Solid arrows labeled A and B refer to marine flooding surfaces. Data symbols in $\delta^{13}C$ profiles: filled square—unaltered dolostone, open square—altered dolostone, filled circle—unaltered limestone, open circle—altered limestone. Altered samples are defined as $\delta^{18}O < -10$ and $Mn/Sr > 10$. The inset illustrates an idealized carbon isotope curve, which is calibrated in absolute time (from Grotzinger et al., 1995; see text for discussion). The dashed lines in the cross section correlate (1) the top of the P-interval and (2) the base of the N-interval. The chemostratigraphic correlations are in agreement with sequence stratigraphic constraints (Pelechaty et al., 1995, 1996). R—Riphean, V—Vendian, ND—Nemakit-Daldyn.

Throughout the Olenek uplift, Vendian strata of the Khorbosuonka Group are <320 m thick and comprise three formations (Sokolov and Fedonkin, 1984; Khomentovsky, 1990; Shenfel, 1991; Pelechaty and Grotzinger, 1993; Knoll et al., 1995a; Fig. 2): the Mastakh Formation, <50 m of conglomerate and dolostone; the Khatyspyt Formation, up to 180 m of black, bituminous limestone; and the Turkut Formation, 80–300 m of buff dolostone. The Mastakh Formation is truncated toward the southern Olenek uplift (sections 2 and 3) where the entire Khorbosuonka Group is represented by the Turkut Formation (Khomentovsky, 1990). In the Kharaulakh Mountains, rocks stratigraphically equivalent to the Khorbosuonka Group are known as the Kharayutekh Formation. They are completely exposed at section 5, and only the upper part of the formation is exposed at section 6. The lower, middle, and upper members of the Kharayutekh Formation contain mixed dolostone, bituminous limestone, and minor siliciclastic rocks and have been interpreted to correlate with the Mastakh, Khatyspyt, and Turkut Formations, respectively (Shapovalova and Shpunt, 1982; Khomentovsky, 1990).

The age of these Vendian strata is tightly constrained. The Khorbosuonka Group contains Ediacaran soft-bodied metazoan fossils in the Khatyspyt Formation (Sokolov and Fedonkin, 1984; Karlova, 1987; Vodanjuk, 1989; Missarzhevsky, 1989; Knoll et al., 1995a) and exhibits $\delta^{13}C$ profiles similar to other latest Vendian intervals (Kaufman et al., 1991; Narbonne et al., 1994; Knoll et al., 1995a; reviewed in Kaufman and Knoll, 1995). The isotopic profile at the Khorbosuonka River contains a lower positive excursion, an interval of isotopic values near 0‰, and an upper negative shift at the top of the Turkut Formation (see section 4 and inset; Fig. 2). Knoll et al. (1995a) correlated the positive isotopic shift through the Mastakh and lower Khatyspyt Formations with a similar positive isotopic excursion in the Zaris Formation of the Nama Group, Namibia. Following this correlation, U-Pb radiometric dates from volcanic ash beds interlayered with sedimentary rocks of the Nama Group allow calibration of the isotopic profiles (Grotzinger et al., 1995) and provide an age of 549 Ma for the top of the positive shift, 544 Ma for the base of the negative shift, and 543 Ma for the top of the negative shift and the Precambrian-Cambrian boundary (see inset; Fig. 2). This age for the boundary is also consistent with an upper-intercept U-Pb age of 543.8 +5.1/–1.3 Ma from a volcanic breccia at the base of the Kessyusa Formation overlying the Khorbosuonka Group (Bowring et al., 1993). The part of the Khorbosuonka Group that exhibits the positive shift is composed of the Mastakh Formation, which forms a single depositional sequence (Knoll et al., 1995a), and the lower Khatyspyt Formation. A maximum age of 555 Ma is estimated for the base of the Khorbosuonka Group on the basis of a conservative overestimate for the time required to form a depositional sequence (Vail et al., 1984; Christie-Blick et al., 1995). Thus, the Khorbosuonka Group and correlative units in northeast Siberia are considered to span a maximum of 10 m.y. during latest Vendian time.

Depositional Facies

Knoll et al. (1995a) described four main carbonate-ramp facies, including tidal flat, lagoon, shoal, and distal, along the Khorbosuonka River (Figs. 1 and 2). Karstic features developed at the top of the Vendian interval truncate most of these facies. Minor siliciclastic deposits of marine and terrestrial origin are present at the base of these sections. These facies are briefly summarized below along with additional sedimentologic and stratigraphic observations from across the Olenek uplift and Kharaulakh Mountains (Pelechaty and Grotzinger, 1993). More detailed facies descriptions are given by Pelechaty et al. (1996).

Tidal Flat Facies. The tidal flat facies (entirely dolostone) is composed mainly of thin-bedded, desiccation-cracked microbial laminites, minor rippled and planar-laminated oolite, and edgewise conglomerate. Early diagenetic chert nodules and white cauliflower chert, which signify the former presence of calcium sulfate evaporites, are only locally developed in the Mastakh Formation (Knoll et al., 1995a).

Lagoon Facies. The lagoon facies (entirely dolostone) is characterized by intercalated thin- to medium-bedded stromatolitic biostromes, rare rudstone, grainstone, and mudstone, and green shale layers between dolostone beds. These deposits have been interpreted to record sedimentation within a low-energy, shallow-water lagoonal setting (Knoll et al., 1995a).

Shoal Facies. The shoal facies comprises mainly trough cross-stratified rudstone, grainstone, and packstone as amalgamated units with sharp, erosive bases. Deposits are intraclastic to oncolitic. Minor stromatolitic biostromes and mudstones form interbeds, signifying incursions of lagoonal conditions in the shoal environment.

Distal Ramp Facies. The distal ramp facies consists of black, bituminous limestone and buff dolostone (mudstone and wackestone). These recessive deposits form nodular beds, massive debris-flow units, and finely laminated distal turbidites (Knoll et al., 1995a). Small-scale flutes and gutter casts, as well as soft-sediment slumps associated with the deposits, are indicative of distal ramp settings. Some of the limestones contain up to 5% total organic carbon. They produce a strong fetid odor when fractured and are considered mature petroleum source units (Chersky, 1986; Bolshakov, 1987). The preservation of ubiquitous organic matter in the limestones indicates that the environment was likely anoxic or had high sedimentation (e.g., North, 1990; Derry et al., 1992).

Karst. Karst facies at the top of the Turkut Formation along the Khorbosuonka River (Knoll et al., 1995a) also extend throughout the Olenek uplift and Kharaulakh Mountains. The paleokarst is represented by an extensive erosion surface with up to 20 m of local relief associated with potholes, shallow sinkholes, karren, and decimetre-scale caves filled with Cambrian sandstone. In the Olenek uplift, typically buff dolostones of the Turkut Formation are stained red owing to the development of terra rossa along this ancient subaerial exposure surface (e.g., Estaban and Klappa, 1983; James and Choquette, 1984; Pelechaty et al., 1991).

Siliciclastic Facies. Minor siliciclastic deposits consist of conglomerate, sandstone, and shale. Trough and hummocky cross-stratified marine sandstone and minor shale of the lower Khatyspyt Formation (section 4; Fig. 2) are also present in the lower Turkut Formation in the southern Olenek uplift, and in the lower Kharayutekh Formation (section 5), where sandstone is intercalated with mud-cracked shale and stromatolitic dolostone of shallow-marine origin (Fig. 2). The lower Mastakh Formation contains up to 10 m of intercalated quartz-pebble conglomerate and sandstone, both showing planar stratification and unidirectional cross-bedding. Beds show abundant truncation and channelization features. Collectively, these attributes are interpreted to signify deposition of channel-floor dunes in braided rivers (e.g., Walker and Cant, 1984).

Stratigraphically, the shallowest-water tidal flat and lagoonal facies are found primarily in the southern Olenek uplift, whereas deeper-water shoal and distal ramp facies dominate sections of the northern Olenek uplift and Kharaulakh Mountains (Fig. 2). The stratigraphic variation of facies is interpreted to record a general northeast platform-to-basin transition (Read, 1983; Grotzinger, 1989).

GEOCHEMISTRY: SAMPLING, ANALYSES, AND RESULTS

Over 320 carbonate samples were evaluated with standard petrographic, cathodoluminescent, and geochemical proxies (e.g., $\delta^{13}C$, $\delta^{18}O$, Fe, Sr, and Mn) to assess diagenetic history and to recognize least-altered samples (Table DR1[1]). The following sections outline

[1]GSA Data Repository item 9642, Table DR1, is available on request from Documents Secretary, GSA, P.O. Box 9140, Boulder, CO 80301.

procedures that were employed for sample collection, laboratory preparation, and analysis.

Sampling and Analytical Procedures

Component (e.g., individual allochems) and whole-rock samples were collected by using a motorized drill equipped with variably sized (2–0.5 mm diameter) drill bits. Whole-rock samples were collected where components were too fine grained for individual sampling. A suite of mainly whole-rock samples were also collected from the lower Kytyngeder River section (section 2 in Fig. 2) in order to test the geochemical variation between whole-rock and component sampling. Whole-rock samples were drilled from areas on thick sections devoid of macroscopic diagenetic fabrics.

Duplicate standard-size thin sections and thick sections (1 mm thick) were made for each component sample. The types of carbonate components that were selected for sampling were determined from plane-light microscopic and cathodoluminescent analyses of thin sections. Sample locations were then spotted on complementary thick sections and drilled. The carbonate composition (e.g., calcite versus dolomite) of samples was determined by using hydrochloric acid in the field and by staining thin sections with Alizarin red-S.

Both depositional and diagenetic components were collected. In some cases, two separate powdered samples were taken from a single thick section (e.g., a depositional and a diagenetic sample, or two separate depositional samples) in order to assess intrasample geochemical variation. For organic-rich carbonate rocks (i.e., black, bituminous limestone), samples of dark, organic-rich layers and light, organic-poor layers were obtained to evaluate isotopic effects related to the alteration of sedimentary organic matter. Depositional components that were sampled included micritic carbonate from massive and laminated detrital sediment (e.g., mudstone and wackestone), intraclasts, oncolitic cortices, and oolitic cortices of packstone, grainstone, and rudstone and from domal to stratiform stromatolites (Table DR1; see footnote 1). Diagenetic components include neomorphic pseudospar and spar and late-stage, void-filling blocky spar and baroque dolomite (e.g., Bathurst, 1975; James and Klappa, 1983; Choquette and James, 1987; Zempolich et al., 1988). These features typically are characterized by high Fe and Mn contents and are dull to nonluminescent.

Procedures for sample preparation and stable isotopic (carbon and oxygen) and major element analyses (Fe, Mn, and Sr) follow those described in detail by Derry et al. (1992) and Narbonne et al. (1994).

Results

The geochemical ($\delta^{13}C$ and $\delta^{18}O$ values and Fe, Mn, and Sr abundances) and petrographic data are summarized in Table DR1 (see footnote 1). Both $\delta^{13}C$ and $\delta^{18}O$ are reported as parts per thousand relative to the Peedee belemnite. Graphically, $\delta^{13}C$ data are plotted as profiles with corresponding stratigraphic sections (Fig. 2), and additional plots are presented to illustrate observed geochemical trends.

Major Element Data. Major element abundance data (Fe, Mn, and Sr) are plotted versus $\delta^{18}O$ in order to evaluate postdepositional alteration (e.g., Brand and Veizer, 1980; Bathurst and Land, 1986; Brasier et al., 1994; Fig. 3). Much of the $\delta^{18}O$ data ranges from –2‰ to –10‰ and shows little variation in either Fe (<5000 ppm) or Mn (<400 ppm) concentration. As expected, the diagenetic components (e.g., burial cement and neomorphic carbonate) are enriched in Fe and Mn (e.g., Grover and Read, 1983; Fig. 3, A and B). Also, dolomudstones of the lower member of the Kharayutekh Formation at section 5 (Fig. 4) are enriched in Fe (up to 19 000 ppm) and Mn (up to 9000 ppm) and exhibit high Mn/Sr ratios and dull to very dull to nonluminescence. These particular depositional components are interpreted to be altered despite minimal recrystallization and lack of evidence for additional $\delta^{18}O$ depletion. This alteration is stratigraphically restricted to the lower part of the Vendian succession and is interpreted to be related to migration of burial fluids along the Riphean-Vendian unconformity. Apart from these diagenetically altered carbonates and other late-burial cements, the lack of correlation of Fe and Mn abundances with $\delta^{18}O$ suggests that throughout this region the depositional components are minimally altered.

Sr abundance is also uncorrelated with $\delta^{18}O$ but varies with depositional facies (Fig. 3, C). The distal ramp limestones (between 200 and 2500 ppm Sr) are enriched in Sr relative to their dolostone counterparts and dolostones of other facies (<200 ppm). Even the distal ramp limestones (i.e., black, bituminous limestone) are enriched compared to the shoal-facies limestones (i.e., oncolitic grainstone and rudstone), which plot together with dolostones. The high Sr concentrations of the distal ramp limestones suggest that these sediments were originally aragonitic in composition (Davis, 1977; James

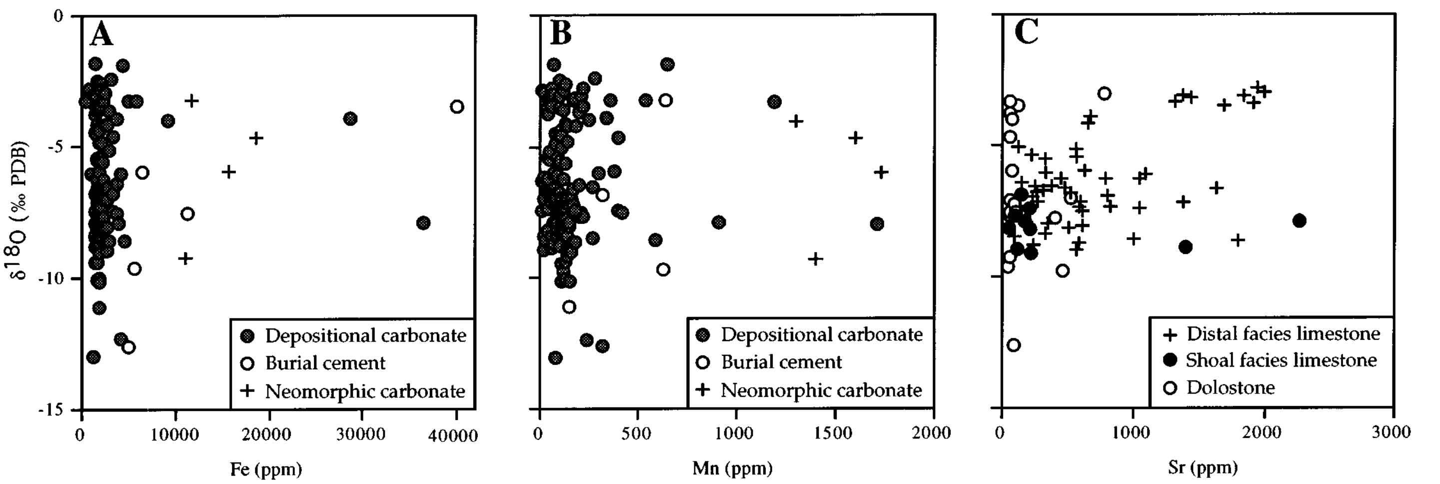

Figure 3. $\delta^{18}O$ versus major element data: (A) Fe and (B) Mn data from all sections, (C) Sr data from the Chekurov anticline (section 5). The diagenetic carbonates (open circles and crosses) in A and B are enriched in both Fe and Mn. Note that the distal ramp limestones in C are enriched in Sr relative to dolostones of all other facies and shoal-facies limestone.

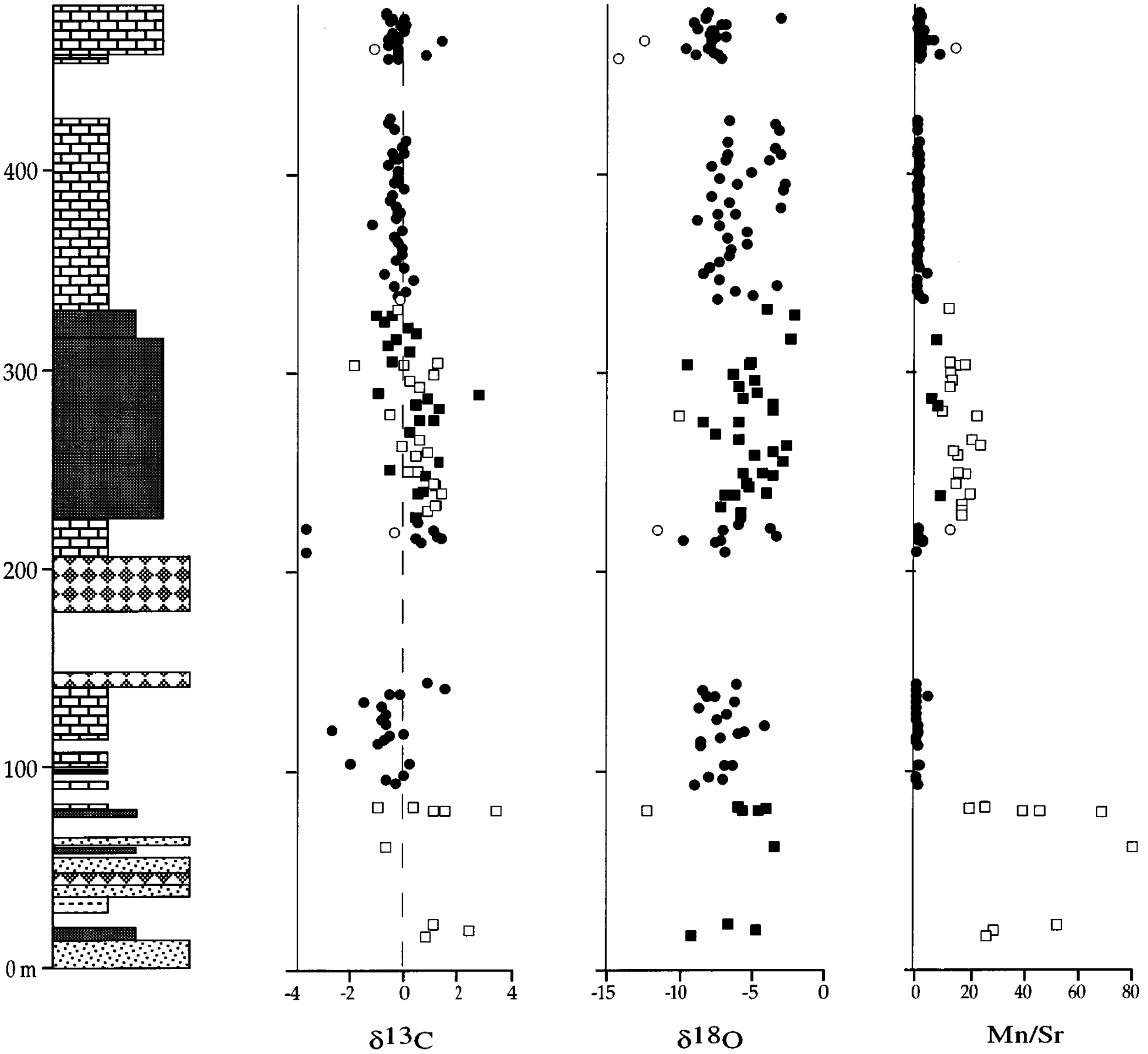

Figure 4. Isotopic and Mn/Sr data from component and diagenetic carbonate for the Chekurov anticline section (profile 5 in Fig. 2). Limestone is shown as bricks and dolostone as shaded regions in the stratigraphic section. Refer to Figure 2 for description of data symbols. On average, dolostones have higher Mn/Sr ratios and heavier carbon isotope values relative to limestones. Not all samples with isotopic values were analyzed for major elements.

and Choquette, 1984; Aissaoui, 1985; Tucker, 1986). The dolomitic distal ramp facies probably lost Sr after deposition through dolomitization. Additional field and petrographic observations further suggest an aragonitic precursor for these limestones. Fabric-selective porosity is typical of carbonates directly beneath the paleokarst at the top of the Turkut and Kharayutekh Formations. Within grainstones and rudstones, porosity formed by selective dissolution of mudstone intraclasts, which form the nuclei of oncoids, while oncoidal rims remain intact. Although now completely dolomitized, selective dissolution strongly suggests that these rocks were bimineralic and that the mudstone intraclasts were composed of a relatively more soluble calcium carbonate form (i.e., aragonite).

$\delta^{13}C$ Profiles. Five $\delta^{13}C$ profiles were constructed from analyses of organic-poor, depositional carbonate components for the Olenek uplift (sections 1, 2, and 3) and Kharaulakh Mountains (sections 5 and 6; Fig. 2). An additional, previously published $\delta^{13}C$ profile by Knoll et al. (1995a) from the Olenek uplift is included (section 4).

The Khorbosuonka River $\delta^{13}C$ profile (section 4; Fig. 2) reveals prominent excursions interpreted as secular variations (Knoll et al., 1995a). The base of the profile is marked by a distinct positive excursion, defined by $\delta^{13}C$ values that rise upsection from near +2‰ to +6‰ through the Mastakh Formation and then decline to values near 0‰ in the lower Khatyspyt Formation. Values through the remainder of the Khatyspyt Formation are variable, ranging between –4‰ and +4‰, with some of the variation likely associated with early organic diagenesis in these bituminous limestones (Knoll et al., 1995a). An upper interval of little change with $\delta^{13}C$ values near 0‰ characterizes the lower Turkut Formation at this section. This is followed by a negative excursion to values near –3‰ beginning ≈20 m below the top of the Turkut Formation.

The Olenek River profile (section 1; Fig. 2) has a $\delta^{13}C$ pattern similar, in some respects, to the profile at the Khorbosuonka River (section 4). The base of the Olenek River profile shows moderately positive $\delta^{13}C$ values (up to +3‰) in the Khatyspyt Formation that decrease at the boundary of the overlying Turkut Formation to 0‰ and remain near that value through the lower 80 m of the formation. A well-defined negative excursion to –3.5‰ begins 50 m beneath the upper Turkut Formation boundary.

The Oolahan Ooekhtekh River profile (section 3; Fig. 2) exhibits $\delta^{13}C$ data that are slightly different from the results in profiles 1 and 4. Positive $\delta^{13}C$ values up to +4‰ mark the base of the section, and these decrease to 0‰ over 50 m of stratigraphic section. Above this, most of the Turkut Formation is characterized by little change in $\delta^{13}C$ with values ranging between –1‰ and –2‰. Unlike $\delta^{13}C$ profiles at sections 1 and 4, this segment contains carbonates that are relatively invariant and consistently depleted in ^{13}C. The top of the section, ≈60 m beneath the upper Turkut Formation boundary, exhibits positive values near +1‰.

The Turkut Formation in the Kytyngeder River profile (section 2; Fig. 2), consisting of primarily whole-rock data, shows greater isotopic variability (ranging between –4‰ and +3‰) than that recognized in the Turkut Formation at section 3 located only 15 km to the north. The upper Kytyngeder River profile includes strata (≈60 m) not exposed along the Oolahan Ooekhtekh River (section 3); isotopic compositions of carbonates here are from component samples and are similar to those in the upper part of section 3 with $\delta^{13}C$ values near +1‰.

The Chekurov anticline profile (section 5; Fig. 2) has a few data points in the lower part of the middle member of the Kharayutekh Formation with values up to +4‰. These are followed upsection by slightly variable $\delta^{13}C$ values that are <0‰ near an 80-m-thick diabase sill. Above this, at the lower contact of the upper member, $\delta^{13}C$ values are near +2‰ and decrease to –1‰ at the top of the section.

The $\delta^{13}C$ values in the Bokursky anticline profile (section 6; Fig. 2) are variably enriched in ^{13}C, ranging between 0‰ and +3.5‰.

These $\delta^{13}C$ profiles are the integrated result of carbon isotope values from a variety of depositional facies. However, facies appear not to influence the isotopic composition of carbonate. Within the invariant isotopic interval (I-interval; see below), all facies have overlapping $\delta^{13}C$ values that range between –2‰ and +2‰ (Fig. 5, A).

DISCUSSION OF GEOCHEMICAL RESULTS: DIAGENETIC MODIFICATION OF $\delta^{13}C$ VALUES

The possibility of diagenetic alteration of $\delta^{13}C$ values of carbonate samples was investigated on various scales, from millimetre-scale variations within samples to kilometre-scale variations across the basin. The following section discusses the possible effects of various diagenetic processes, including organic diagenesis, dolomitization, meteoric diagenesis, contact-metamorphic effects, and burial diagenesis.

Organic-Matter Diagenesis

Bituminous limestones and uncommon dolostones of distal ramp facies contain abundant organic carbon as dark interstitial material. In several cases, both organic-rich and organic-poor subsamples were collected from the same hand specimen (Table 1). In most cases, organic-rich portions of samples are depleted in ^{13}C relative to their organic-poor counterparts. This depletion is generally interpreted to record the incorporation of carbonate formed during the in situ oxidation of organic matter, a process that produces isotopically light CO_2 (Irwin et al., 1977). Some variation in $\delta^{13}C$ values through the Khatyspyt Formation at section 4 (Knoll et al., 1995a) and the Kharayutekh Formation at sections 5 and 6 may also be related to this process.

Dolomitization

In some cases, $\delta^{13}C$ variations appear to be related to the distribution of limestone and dolostone in these sections, rather than to temporal changes in the isotopic composition of seawater. For example, the $\delta^{13}C$ variation shown in the middle and upper members of the Kharayutekh Formation in the profile at section 5 is correlated with the distribution of carbonate minerals (Figs. 2, 4, and 5, B). In general, the limestones in this section are depleted in ^{13}C relative to dolostones. At least four interpretations can be used to explain these variations.

1. The distribution of limestones stratigraphically above and below the dolostones in this section is coincident with small-scale secular variations in seawater $\delta^{13}C$.

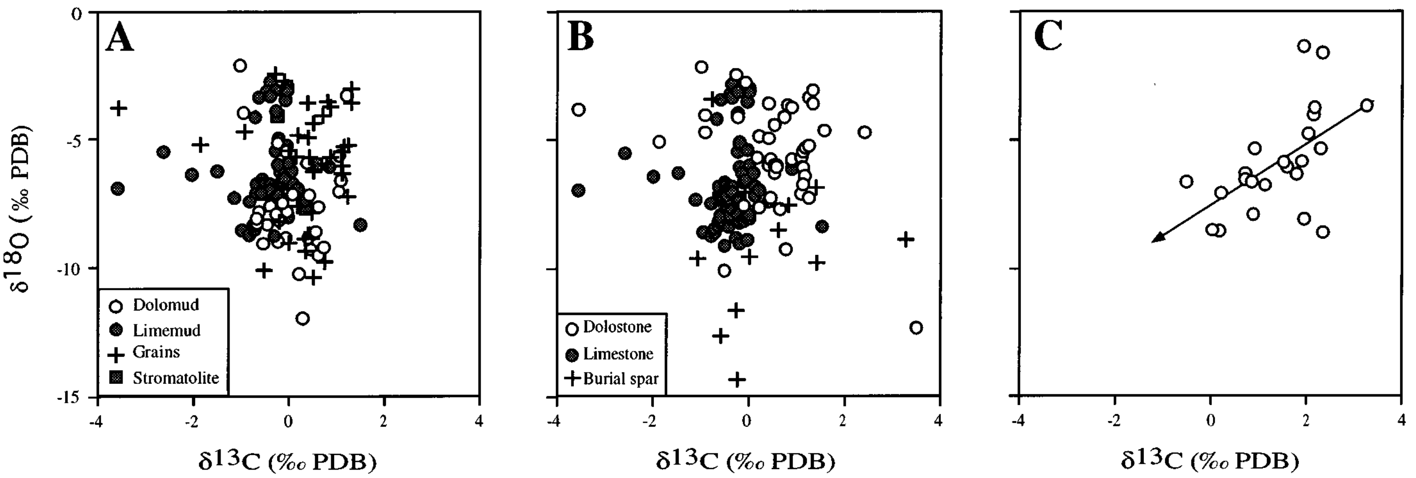

Figure 5. $\delta^{13}C$ versus $\delta^{18}O$ plots: (A) Component data from all the sections are plotted from only the I-interval in order to remove the effect of secular variation. (B) Isotopic data from the Chekurov anticline (section 5); on average, dolostones are enriched relative to limestones. (C) Bokursky anticline data (section 6) suggest a diagenetic trend toward depleted $\delta^{13}C$ and $\delta^{18}O$ values (arrow); this plot shows that the double-positive shift (shown in Fig. 2) may be an altered I-interval with values near +2‰ through the entire profile.

TABLE 1. ISOTOPIC COMPARISON OF ORGANIC-RICH AND ORGANIC-POOR CARBONATE

Number	A Organic-rich sample		B Organic-poor sample		A – B
	$\delta^{13}C$	$\delta^{18}O$	$\delta^{13}C$	$\delta^{18}O$	
KHA 12b,a	–2.0	–6.4	0.2	–6.9	–2.2
KHA 36a,b	0.5	–6.3	1.4	–6.9	–0.9
KHA 41b,a	0.2	–5.6	0.5	–4.4	–0.3
KHA 67a,b	–0.4	N.D.	–1.0	–2.2	0.6
KHA 89a,b	–0.4	–2.8	–0.2	–6.1	–0.2
KHA 93a,b	–0.2	–3.9	–0.4	–7.0	0.2
KHA 94b,a	0.0	–3.1	–0.4	–6.8	0.4
KFC 15a,b	1.5	–5.9	2.3	–5.3	–0.8
KFC 16a,b	2.0	–4.7	2.3	–1.6	–0.3
KFC 19a,b	2.1	–4.0	3.3	–3.7	–1.2
KFC 21a,b	1.9	–8.0	2.3	–8.6	–0.4

Note: N.D.—not determined.

2. The observed isotopic trend could be a signal of depth-dependent variations in ancient seawater ^{13}C. Modern oceans do show a negative gradient in $\delta^{13}C$ with depth, which is recorded in carbonates precipitated along this gradient. Surface waters are enriched in ^{13}C owing to uptake and removal of ^{12}C during photosynthetic production of biomass (Berger and Vincent, 1986); oxidation of isotopically light organic matter at depth additionally enhances the seawater's carbon isotope gradient. In the upper member of the Kharayutekh Formation at section 5, the occurrence of shallow-water dolostones and deep-water limestones suggest depth-dependent variations. However, at the top of the formation, both shallow- and deep-water limestones occur, and both have similar $\delta^{13}C$ values. The lack of absolute constraints on water depths and samples of coeval deposits representative of varying water depths makes it difficult to determine whether an isotopic gradient existed in seawater at this time. Nonetheless, given the existing data, it seems unlikely that depth-dependent variations are controlling the isotopic differences between limestones and dolostones.

3. The isotopic difference could be related to the authigenic formation of dolomite directly from Vendian seawater. Sheppard and Schwarcz (1970) inferred, on the basis of results of high-temperature experiments, that at the temperatures of sedimentary conditions, dolomite is enriched in ^{13}C by as much as 2‰–3‰ relative to calcite, if both phases are in isotopic equilibrium. For an equilibrium isotope effect to have resulted in the present distribution of $\delta^{13}C$ values would require that both calcite and dolomite precipitated from seawater with a constant carbon isotope composition. Ooids within tidal flat facies dolostones exhibit well-preserved, concentrically laminated, cortical fabrics suggestive of having originally been calcite (e.g., Tucker, 1983). This observation suggests that the dolomite in these sections is secondary and argues against the suggestion that limestone and dolostone may have formed contemporaneously.

4. Last, it is possible that differences in $\delta^{13}C$ values in this section and elsewhere in the basin may be related to secondary dolomitization, such that these samples now more closely reflect the isotopic composition of the dolomitizing fluids. In particular, secondary dolomitization may have occurred in section 5 where dolostones have high Mn/Sr ratios and are enriched in $\delta^{13}C$ relative to the limestones in the same section (Figs. 2 and 4). A few studies have demonstrated that dolomitization can lead to enrichment of ^{13}C. For example, reflux-style dolomitization of limestone in the presence of brines enriched in ^{13}C through anaerobic fermentation (i.e., methanogenesis) has been interpreted to result in a positive offset of primary $\delta^{13}C$ values of dolomitic samples from Paleozoic reefs (Sears and Lucia, 1980; Cercone and Lohmann, 1987). The offset is caused by the addition of newly formed dolomite with compositions significantly enriched in ^{13}C. Although incorporation of even small amounts of CO_2 formed as a byproduct of bacterial methanogenesis can alter $\delta^{13}C$ values of sediments, it seems unlikely that this process would affect every sample in a succession to the same degree.

Meteoric Diagenesis

In carbonate-dominated successions, meteoric diagenesis is common and has been found elsewhere to modify the isotopic and elemental composition of carbonate. Following earlier studies (e.g., Knoll et al., 1995a), samples with Mn/Sr >10‰ and $\delta^{18}O$ <–10‰ are defined as having been altered. Permeable limestones, particularly those interbedded with siliciclastic rocks, can be altered by such meteoric diagenesis, e.g., the basal part of the Kharayutekh Formation (Figs. 2 and 4). The stratigraphic significance of these isotopic compositions is interpreted with caution. On the other hand, thick limestone units from this basin are considered unaltered on the basis of low Mn/Sr values, high Sr abundances, and little-altered $\delta^{18}O$ values. The $\delta^{13}C$ values from these facies are interpreted to record primary secular variations.

Karst-related diagenesis has been found elsewhere to alter the isotopic composition of carbonate. In this case, fluids are enriched in ^{18}O through evaporation and depleted in ^{13}C by the addition of soil CO_2 (Allen and Matthews, 1982; Beeunas and Knauth, 1985). However, although negative trends in $\delta^{13}C$ values are seen in sections 1 and 4 (Fig. 2), no trend is noted in the other sections immediately beneath the paleokarst. Also, there is no discernible variation in the $\delta^{18}O$ values of samples approaching this basinwide exposure surface (Fig. 6). The negative $\delta^{13}C$ excursion seen in a few of these northern Siberian profiles also have been noted in Precambrian-Cambrian boundary sections from southern Siberia, Morocco, northwest Canada, China, and Iran (summarized in Kaufman and Knoll, 1995) where no exposure surfaces have been recognized. The $\delta^{13}C$ excursions in these sections are all interpreted as records of secular variation rather than diagenetic alteration.

Contact-Metamorphic Effects

High-temperature effects associated with igneous bodies appear to deplete carbonate with respect to ^{13}C and ^{18}O. The isotopic effects of diabase intrusion may be evident in section 5 (Fig. 2) in the lower part of the Kharayutekh Formation. The carbonates near the sills are depleted in ^{13}C but have $\delta^{18}O$ values similar to carbonates throughout the section (Figs. 2, 4, and 6).

At section 6, outcrops of dolostones are highly altered and show internal brecciation and development of crackle breccia, with fractures and intrablock zones filled with very coarse crystalline spar. This style of alteration is often attributed to hydrothermal activity, which may result in significant isotopic alteration (see covariance of ^{13}C and ^{18}O; Fig. 5, C). An unaltered version of this profile may have consisted of all values near +2‰, which may represent the invariant isotopic interval (i.e., the I-interval; see below) between the lower positive and upper negative shifts. High-temperature alteration of these carbonates may have occurred in earliest Cambrian time during extrusion of basaltic lavas now present in the lower Tyuser Formation overlying the Vendian carbonates (Vidal et al., 1995). Lacking elemental data for these samples, we are unable to evaluate further any effects of diagenetic alteration, but we view the $\delta^{13}C$ values with caution.

Burial Diagenesis

Subsamples taken from hand specimens show that burial precipitates are systematically de-

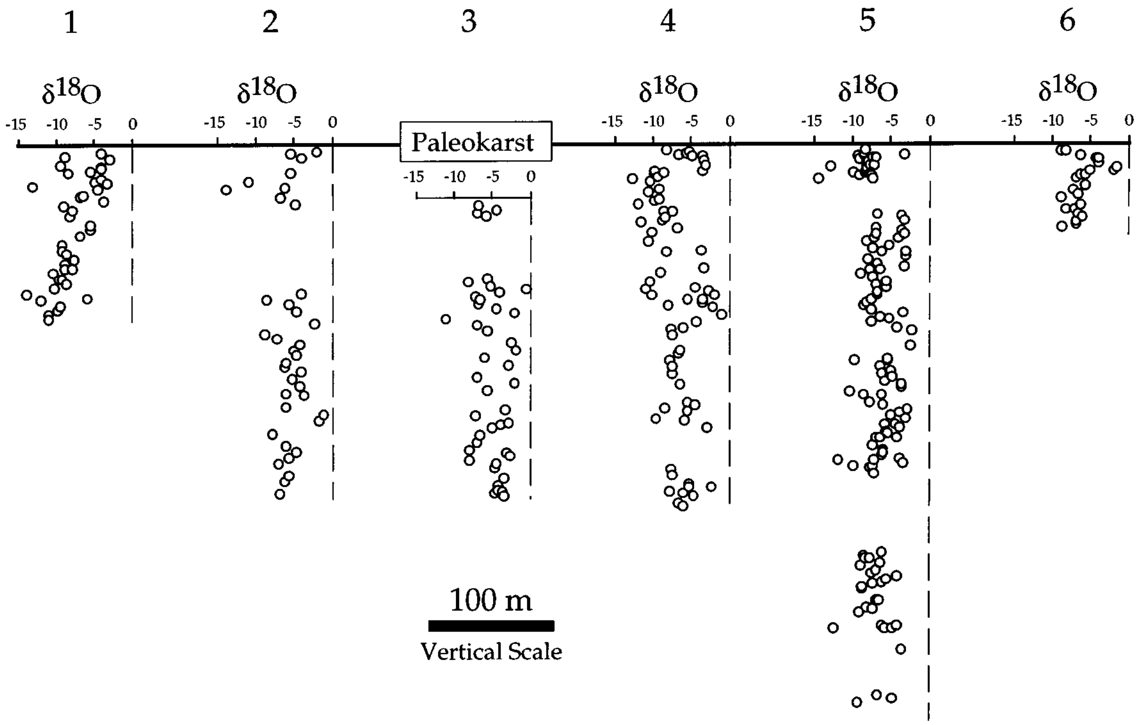

Figure 6. Plots of δ18O versus depth for stratigraphic sections (refer to Fig. 1 for location of sections) in the Olenek uplift and Kharaulakh Mountains. The horizontal datum represents the paleokarst unconformity at the top of the Turkut and Kharayutekh Formations.

pleted in ^{18}O relative to marine depositional components (Fig. 5, B; Table 2), which is typical of diagenetically altered carbonate (Lohmann, 1982; Arthur et al., 1983; Grover and Read, 1983; Choquette and James, 1987). However, there seems to be no preferential change in ^{13}C of depositional components relative to burial cements (Table 2).

INTEGRATION OF GEOLOGIC AND GEOCHEMICAL DATA

Correlation of the δ^{13}C Profiles

For the purpose of intrabasinal correlation, the terminal Vendian δ^{13}C chemostratigraphic record in northeast Siberia is divided into three isotopically defined intervals. In the order of decreasing age (see inset in Fig. 2), these intervals are characterized by a positive shift (P-interval), an interval of relatively invariant isotopic composition (I-interval), and a negative shift (N-interval).

Correlation of the δ^{13}C profiles of the Olenek uplift and Kharaulakh Mountains is based on integration of both the isotopic data and regional stratigraphic and sedimentologic trends. The proposed chemostratigraphic correlation is also supported by sequence stratigraphic correlation of these same sections, which is described elsewhere (Pelechaty et al., 1995, 1996). The most complete δ^{13}C record in this region is the one shown by the profile at section 4 (Fig. 2; Knoll et al., 1995a); this profile exhibits distinct, large-magnitude oscillations ideal for chemostratigraphic correlation and includes all three isotopic intervals.

The P-interval is well developed in section 4 through the Mastakh and lower Khatyspyt Formations and is interpreted to correlate with the basal positive excursions at sections 1, 2, and 3 in the Olenek uplift area. The P-interval in section 4 is less confidently correlated with the basal part of the middle member of the Kharayutekh Formation at section 5 where the excursion is defined by only a few data points. Correlation of these positive shifts is supported stratigraphically by the recognition of a significant marine flooding surface (A in Fig. 2) at this level, defined by a sharp transition from shallow-water dolostones to black, bituminous limestones of the distal ramp facies that can be correlated throughout this region.

The I-interval is developed across the basin but varies greatly in its stratigraphic thickness. The I-interval at section 4 is correlated with similar intervals at sections 1, 2, and 3 in the Olenek uplift; in the Kharaulakh Mountains,

TABLE 2. ISOTOPIC COMPARISON OF DEPOSITIONAL AND DIAGENETIC COMPONENTS WITHIN SAMPLES

Number	A Diagenetic components*		B Depositional components		A – B
	δ^{13}C	δ^{18}O	δ^{13}C	δ^{18}O	
KHA 6ab,aa	3.5	–12.3	1.5	–4.6	2.0
KHA 24,b	–0.5	–7.7	–0.1	–8.2	–0.4
KHA 28a,bb	1.4	–9.8	0.6	–7.7	0.8
KHA 30,b	–0.3	–11.7	1.0	–7.1	–1.3
KHA 49a,b	0.6	–8.5	1.1	–10.1	–0.5
KHA 58a,b	0.0	–9.5	–1.9	–5.2	1.9
KHA 84a,b	–0.3	–7.5	–0.2	–6.2	–0.1
KHA 100,b	–0.2	–14.3	–0.6	–7.2	0.4
KHA 103b,a	–1.1	–9.7	–0.2	–8.2	–0.9
KHA 105a,b	1.4	N.D.	–0.2	–7.9	1.6
KHA 107a,b	–0.2	–7.0	–0.4	–7.7	0.2
KHA 109a,b	0.0	–7.8	0.0	–7.9	0.0
KHA 111a,b	–0.2	–6.9	0.1	–3.1	–0.3
KFC 6a,b	0.9	–7.9	1.1	–6.7	–0.2

Note: N.D.—not determined.
*Diagenetic components include pseudospar, spar, and baroque dolomite.

with almost the entire isotopic profile at section 5; and with the profile at section 6, where the $\delta^{13}C$ data are interpreted to reflect an altered primary signal (Figs. 2 and 5, C). This correlation reveals pronounced thickening of the I-interval from 75 m at section 1, to 200 m at section 4, and to at least 420 m at section 5 (the N-interval is not preserved at section 5, where the total stratigraphic thickness of the I-interval is unknown). The I-interval at section 6 probably correlates with part of the I-interval in the upper member of the Kharayutekh Formation at section 5 on the basis of correlation of additional prominent flooding surfaces in both sections (B in Fig. 2). Because of variations in facies, minerals, igneous activity, and diagenesis across the basin, it is unclear whether the small-scale variations in the I-interval reflect secular variation and/or diagenetic alterations.

Overlying the I-interval, the N-interval is well developed only at sections 1 and 4. In general, the isotopic intervals appear to be progressively truncated beneath the paleokarst capping the Turkut and Kharayutekh Formations from section 1 toward section 6.

Depositional Effects on $\delta^{13}C$ Excursions

The geometry of the $\delta^{13}C$ profiles is considered to record variations in the long-term sediment-accumulation rate (as a proxy for subsidence rate) and the distribution and magnitude of hiatuses within the sedimentary basin. These effects have not received much prior attention because of a primary focus on intercontinental rather than intrabasinal correlations.

Sediment-Accumulation Rate. The obvious effect of sediment-accumulation rate on the ^{13}C isotopic record is to modify the general form of isotopic excursions. Areas of low sediment accumulation show a condensed record, in some cases with abrupt isotopic changes. In contrast, sites of high sediment accumulation are marked by isotopic profiles with generally smoother isotopic variations. For the shallow-water carbonates discussed here, where variations in depositional water depth (less than tens of metres) are small relative to the thickness of the deposits (hundreds of metres), sediment-accumulation rate is considered to be related to variations in the rate of tectonic subsidence (Schlager, 1981; Sadler, 1981). In particular, in this basin, I-interval strata accumulated either entirely near sea level (sections 2 and 3) or shoaled to sea level at the close of I-interval time (sections 1, 4, and 5).

Relative to the P-interval and N-interval at the base and top of these sections, respectively, the I-interval has been considered a significant isotopic interval that occupies a thick portion of the Vendian stratigraphic record (e.g., Knoll and Walter, 1992; Narbonne et al., 1994; Knoll et al., 1995a). The significance of the I-interval, in terms of rock thickness, varies across the Olenek uplift and Kharaulakh Mountains and is interpreted to reflect variations in sediment-accumulation rate. Subsidence increased toward the Kharaulakh Mountains during P-interval and I-interval times. Section 1 is located farthest to the west, and its strata indicate that this part of the basin was associated with, on average, lower subsidence rates. The basin underwent eastward-increasing subsidence from the eastern Olenek uplift to the Kharaulakh Mountains at section 5. This interpretation is consistent with the regional platform-to-basin transition: mainly tidal flat facies in the southern Olenek area but mixed shoal and distal ramp facies farther eastward.

The observed subsidence pattern during I-interval time shows that rates were relatively lower at section 1 but greater to the south (sections 2 and 3) and east (section 4) over a distance of 45 km. The regions of greater subsidence show contrasting depositional responses. To the south, at sections 2 and 3, tidal-flat sediments appear to have accumulated at rates equal to rates of local subsidence, whereas to the east at section 4, subsidence outpaced sediment accumulation, causing drowning of the platform and deposition of deeper-water, outer-ramp sediments, followed by shoaling.

The intervening region at section 1 may represent a foreland bulge. However, the spatial dimensions of the postulated tectonic bulge approach the lower size limits of other peripheral bulges (Karner and Watts, 1983; Waschbusch and Royden, 1992; McCormick and Grotzinger, 1992). Section 1 is located farthest to the west and may partially reflect onlap onto the craton in a region of lower subsidence during I-interval time. This interpretation is further supported by unpublished seismic profiles that show westward thinning of Vendian strata. Local synsedimentary block faulting may also have led to complex subsidence patterns observed in the Olenek uplift (e.g., Bechstädt and Boni, 1989) during N-interval time near the close of the Vendian and during development of the unconformity that caps the Turkut and Kharayutekh Formations.

Hiatuses. The distribution and magnitude of depositional hiatuses within the stratigraphic record are complex and represent much geologic time (Sadler, 1981; Anders et al., 1987). This attribute of the stratigraphic record adds a distinct randomness to preservation of isotopic events, which affects both form and magnitude of carbon isotope excursions. In northeast Siberia, the paleokarst unconformity that caps the Turkut and Kharayutekh Formations is a prominent hiatal surface that shows systematic variations in the amount of erosion throughout the Olenek uplift and Kharaulakh Mountains area. This erosion has had the effect of partially erasing the carbon isotope record. The $\delta^{13}C$ profiles show progressive downcutting of the Turkut and equivalent strata from section 1 toward the southern Olenek uplift and toward the Kharaulakh Mountains where erosion has removed strata well beneath any deposits of N-interval age (section 6).

The unconformity defining the top of the Turkut and Kharayutekh Formations also variably truncates Vendian strata across the Siberian platform according to the results of a comparison of carbon isotope profiles. This unconformity is expressed throughout the eastern Siberian platform as either a well-developed paleokarst or as a subtle stratigraphic surface (Khomentovsky, 1990). Erosion along this surface appears to have been more pronounced in northern Siberia than in the south. The N-interval is variably truncated across the north, from the western Anabar region (Pokrovsky and Venagradov, 1991; Pokrovsky and Missarzhevsky, 1993; Knoll et al., 1995b) to the Kharaulakh Mountains, whereas to the south, a complete N-interval, with values that return to 0‰ at the top of Vendian strata, is developed at sections along the Lena and Aldan Rivers (Magaritz et al., 1986, 1991; Kirschvink et al., 1991; Brasier et al., 1994).

CONCLUSIONS

Latest Vendian carbonate-dominated strata of the Olenek uplift and Kharaulakh Mountains in northeast Siberia provide a unique opportunity to examine variations between many $\delta^{13}C$ profiles within a single sedimentary basin. These carbon isotope profiles record secular oscillations in $\delta^{13}C$, as well as secondary signals. The Vendian strata in this region exhibit three prominent secular isotopic events, which are observed in several other basins worldwide: an older positive shift (P-interval) with values up to +6‰, an invariant interval (I-interval) with values between +1‰ and –2‰, and a younger negative shift (N-interval) characterized by values to –4‰.

Both the magnitude and form of these secular oscillations vary from profile to profile and are considered to reflect the effects of diagenetic and depositional processes. A variety of early- to late-stage diagenetic processes (i.e., organic-matter diagenesis, dolomitization, burial diagenesis, and contact-metamorphic effects) may alter the magnitude of the secular shifts, a fact that is well displayed between limestone and dolostone at some sections. The small-scale isotopic variation observed in the I-interval in this basin probably reflects both secular and diagenetic signals. However, further investigation of stratigraphic sections through the I-interval is needed to distinguish between secular and local signals.

Geologic processes modify the recorded pattern of primary isotopic shifts. For instance, variations in subsidence rate affect the stratigraphic thickness that preserves isotopic events, whereas erosion truncates isotopic signals at unconformities. These complications imply that the carbon isotope profiles from other parts of the Siberian platform, and from other sedimentary basins, may be missing key isotopic events, or partial events may be spliced together and form complex, incomplete records.

Because of the variability of carbon isotope records within a sedimentary basin, additional geochemical, sedimentologic, and stratigraphic data are required to unravel complexities of diagenesis and basin dynamics and their effects on the preservation of primary carbon isotope values preserved in carbonate. However, despite small-scale complications provided by nonsecular isotopic signals preserved within carbon isotope profiles, chemostratigraphy provides a useful method for high-resolution intrabasinal correlation, and resolving basin dynamics (see Pelechaty et al., 1996; Pelechaty, 1996).

ACKNOWLEDGMENTS

Funding for this project was provided by Maxus Energy Corporation, Dallas, National Science Foundation (NSF) grant EAR-9058199 to Grotzinger, and NSF BSR-90-17747 grant to A. H. Knoll for Kaufman. Yakutsk Geophysics, Republic of Yakutia, is thanked for providing logistical support to Pelechaty for three field seasons. We especially thank V. P. Zhernovsky, V. A. Kashirtsev, P. N. Kolosov, L. Niemi, and A. Bailekh for invaluable field assistance. We thank Stein Jacobsen for support and access to the Harvard laboratories. We appreciated the insightful comments of A. H. Knoll and B. Z. Saylor, and we thank Journal reviewers N. Christie-Blick, M. D. Brasier, and M. R. Walter for their reviews.

REFERENCES CITED

Aissaoui, D. M., 1985, Botryoidal aragonite and its diagenesis: Sedimentology, v. 32, p. 345–362.

Allen, J. R., and Matthews, R. K., 1982, Isotope signatures associated with early meteoric diagenesis: Sedimentology, v. 29, p. 797–817.

Anders, M. H., Krueger, S. W., and Sadler, P. M., 1987, A new look at sedimentation rates and the completeness of the stratigraphic record: Journal of Geology, v. 95, p. 1–14.

Arthur, M. A., Anderson, T. F., Kaplan, I. R., Veizer, J., and Land, L. S., 1983, Stable isotopes in sedimentary geology: Society of Economic Paleontologists and Mineralogists Short Course 10, 435 p.

Bathurst, R. G. C., 1975, Carbonate sediments and their diagenesis: Amsterdam, Elsevier Scientific Publication Co., Developments in Sedimentology 12, 658 p.

Bathurst, R. G. C., and Land, L. S., 1986, Part 5: Diagenesis 1, *in* Warme, J. E., and Stanley, K. W., eds., Carbonate depositional environments: Modern and ancient: Colorado School of Mines Quarterly, v. 81, p. 1–41.

Bechstädt, T., and Boni, M., 1989, Tectonic control on the formation of a carbonate platform: The Cambrian of southwestern Sardinia, *in* Crevello, P. D., Wilson, J. L., Sarg, J. F., and Read, J. F., eds., Controls on carbonate platform and basin development: Society for Sedimentary Geology (SEPM) Special Publication 44, p. 107–122.

Beeunas, M. A., and Knauth, L. P., 1985, Preserved stable isotope signatures of subaerial diagenesis in the 1.2 Ga Mescal Limestone, central Arizona: Implications for the timing and development of a terrestrial plant cover: Geological Society of America Bulletin, v. 96, p. 737–745.

Berger, W. H., and Vincent, E., 1986, Deep-sea carbonates: Reading the carbon isotope signal: Geologisches Rundschau, v. 75, p. 249–269.

Bolshakov, Y. A., 1987, Geology and geochemistry of oil and gas, and coal, Yakutia: Yakutia, Russian Academy of Sciences, 143 p. (in Russian).

Bowring, S. A., Grotzinger, J. P., Isachsen, C. E., Knoll, A. H., Pelechaty, S. M., and Kolosov, P., 1993, Calibrating rates of Early Cambrian evolution: Science, v. 261, p. 1293–1298.

Brand, U., and Veizer, J., 1980, Chemical diagenesis of a multicomponent system—1. Trace elements: Journal of Sedimentary Petrology, v. 50, p. 1219–1236.

Brasier, M. D., Khomentovsky, V. V., and Corfield, R. M., 1993, Stable isotopic calibration of the earliest skeletal fossil assemblages in eastern Siberia (Precambrian-Cambrian boundary): Terra Nova, v. 5, p. 225–232.

Brasier, M. D., Corfield, R. M., Derry, L. A., Rozanov, A. Y., and Zhuravlev, A. Y., 1994, Multiple $\delta^{13}C$ excursions spanning the Cambrian explosion to the Botomian crisis in Siberia: Geology, v. 22, p. 455–458.

Cercone, K. R., and Lohmann, K. C., 1987, Early diagenesis of middle Silurian pinnacle reefs, northern Michigan, *in* Cercone, K. R., and Budai, J. M., eds.: Ordovician and Silurian rocks of the Michigan basin and its margins: Michigan Basin Geological Society Special Publication 4, p. 109–130.

Chersky, H. V., 1986, Upper Precambrian–Phanerozoic oil and gas deposits, eastern part of the Siberian platform: Yakutia, Russian Academy of Sciences, 123 p. (in Russian).

Choquette, P. W., and James, N. P., 1987, Diagenesis no. 12. Diagenesis in Limestones—3. The deep burial environment: Geoscience Canada, v. 14, p. 3–35.

Christie-Blick, N., Dyson, I. A., and von der Borch, C. C., 1995, Sequence stratigraphy and the interpretation of Neoproterozoic earth history: Precambrian Research, v. 73, p. 3–26.

Davis, G. R., 1977, Former magnesium calcite and aragonitic submarine cements in upper Paleozoic reefs of the Canadian Arctic: Geology, v. 5, p. 11–15.

Derry, L. A., Kaufman, A. J., and Jacobsen, S. B., 1992, Sedimentary cycling and environmental change in the Late Proterozoic: Evidence from stable and radiogenic isotopes: Geochimica et Cosmochimica Acta, v. 56, p. 1317–1329.

Estaban, M., and Klappa, C. F., 1983, Subaerial exposure, *in* Scholle, P. A., Bebout, D. G., and Moore, C. H., eds., Carbonate depositional environments: American Association of Petroleum Geologists Memoir 33, p. 1–93.

Grotzinger, J. P., 1989, Facies and evolution of Precambrian carbonate depositional systems: Emergence of the modern platform archetype, *in* Crevello, P. D., Wilson, J. L., Sarg, J. F., and Read, J. F., eds., Controls on carbonate platform and basin development: Society for Sedimentary Geology (SEPM) Special Publication 44, p. 79–106.

Grotzinger, J. P., Bowring, S. A., Saylor, B. Z., and Kaufman, A. J., 1995, Biostratigraphic and geochronologic constraints on early animal evolution: Science, v. 270, p. 598–604.

Grover, G. J., and Read, J. F., 1983, Paleoaquifer and deep-burial related cements defined by regional cathodoluminescence patterns, Middle Ordovician carbonates, Virginia: American Association of Petroleum Geologists Bulletin, v. 67, p. 1275–1303.

Harland, B. W., Armstrong, R. L., Cox, A. V., Smith, A. G., and Smith, D. G., 1989, A geologic time scale: Cambridge, Cambridge University Press, 263 p.

Irwin, H., Curtis, C., and Coleman, M., 1977, Isotopic evidence for source of diagenetic carbonates formed during burial of organic-rich sediments: Nature, v. 269, p. 209–213.

James, N. P., and Choquette, P. W., 1984, Diagenesis 9. Limestones—The meteoric diagenetic environment: Geoscience Canada, v. 11, p. 161–194.

James, N. P., and Klappa, C. F., 1983, Petrogenesis of Early Cambrian reef limestones, Labrador: Canada: Journal of Sedimentary Petrology, v. 53, p. 1051–1096.

Karlova, G. A., 1987, First findings of skeletal fauna in the Turkut Formation of the Olenek uplift: Doklady Academica Science USSR, v. 292, p. 204–205 (in Russian).

Karner, G. D., and Watts, A. B., 1983, Gravity anomalies and flexure of the lithosphere at mountain ranges: Journal of Geophysical Research, v. 88, p. 10449–10477.

Kaufman, A. J., and Knoll, A. H., 1995, Neoproterozoic variations in the C-isotopic composition of seawater: Stratigraphic and biogeochemical implications: Precambrian Research, v. 73, p. 27–49.

Kaufman, A. J., Hayes, J. M., Knoll, A. H., and Germs, G. J. B., 1991, Isotopic compositions of carbonates and organic carbon from upper Proterozoic successions in Namibia: Stratigraphic variation and the effects of diagenesis and metamorphism: Precambrian Research, v. 49, p. 301–327.

Khomentovsky, V. V., 1990, Chapter 5: Vendian of the Siberian Platform, *in* Sokolov, B. S., and Fedonkin, M. A., eds., Regional geology: The Vendian System: Berlin, Springer-Verlag, v. 2, p. 103–183.

Khomentovsky, V. V., and Karlova, G. A., 1993, Biostratigraphy of the Vendian–Cambrian beds and the Lower Cambrian boundary in Siberia: Geological Magazine, v. 130, p. 29–45.

Kirschvink, J. L., Magaritz, M., Ripperdan, R. L., Zhuravlev, A. Y., and Rozanov, A. Y., 1991, The Precambrian-Cambrian boundary: Magnetostratigraphy and carbon isotopes resolve correlation problems between Siberia, Morocco, and south China: GSA Today, v. 1, p. 69–71, 87, 91.

Knoll, A. H., and Walter, M. R., 1992, Latest Proterozoic stratigraphy and Earth history: Nature, v. 356, p. 673–678.

Knoll, A. H., Grotzinger, J. P., Kaufman, A. J., and Kolosov, P., 1995a, Integrated approaches to terminal Proterozoic stratigraphy: An example from the Olenek uplift, northeastern Siberia: Precambrian Research, v. 73, p. 251–270.

Knoll, A. H., Kaufman, A. J., Semikatov, M. A., Grotzinger, J. P., and Adams, W. E., 1995b, Sizing up the sub-Tommotian unconformity in Siberia: Geology, v. 23, p. 1139–1143.

Krasilshchikov, A. A., and Biterman, I. M., 1970, Proterozoic group of the Olenek uplift, *in* Markov, F. G., ed., Geology of the USSR western part of the Yakutian ASSR: Nedra, p. 91–100 (in Russian).

Lambert, I. B., Walter, M. R., Wenlong Z., Songnian Lu, and Guogan Ma, 1987, Paleoenvironmental and carbon isotope stratigraphy of upper Proterozoic carbonates of the Yangtze Platform: Nature, v. 325, p. 140–142.

Lohmann, K. C., 1982, Inverted J carbon and oxygen isotopic trends—Criteria for shallow meteoric phreatic diagenesis: Geological Society of America Abstracts with Programs, v. 14, p. 548.

Magaritz, M., Hoser, W. T., and Kirschvink, J. L., 1986, Carbon-isotope events across the Precambrian-Cambrian boundary on the Siberian platform: Nature, v. 320, p. 258–259.

Magaritz, M., Kirschvink, J. L., Latham, A., Zhuravlev, A. Y., and Rozanov, A. Y., 1991, Precambrian-Cambrian boundary problem: Carbon isotope correlations for Vendian and Tommotian time between Siberia and Morocco: Geology, v. 19, p. 847–850.

McCormick, D. S., and Grotzinger, J. P., 1992, Evolution and significance of an overfilled alluvial foreland basin: Burnside Formation (1.9 Ga), Kilohigok Basin, N.W.T., Canada: Basin Research, v. 4, p. 253–278.

Missarzhevsky, V. V., 1989, Oldest skeletal fossils and stratigraphy of Precambrian and Cambrian boundary beds: Nauka, v. 221, p. (in Russian).

Narbonne, G. M., Kaufman, A. J., and Knoll, A. H., 1994, Integrated chemostratigraphy and biostratigraphy of the upper Windermere Supergroup (Neoproterozoic), Mackenzie Mountains, northwestern Canada: Geological Society of America Bulletin, v. 106, p. 1281–1292.

North, F. K., 1990, Petroleum geology: Boston, Unwin Hyman, 631 p.

Pelechaty, S. M., 1996, Stratigraphic evidence for the Siberia-Laurentia connection and Early Cambrian rifting: Geology, v. 24, p. 719–722.

Pelechaty, S. M., and Grotzinger, J. P., 1993, Correlation of Vendian carbonate rocks between the Olenek uplift and Kharaulakh Mountains, northern Siberia: Geological Society of America Abstracts with Programs, v. 25, p. A337.

Pelechaty, S. M., James, N. P., Kerans, C., and Grotzinger, J. P., 1991, A Middle Proterozoic paleokarst unconformity and associated sedimentary rocks, Elu Basin, northwest Canada: Sedimentology, v. 38, p. 775–797.

Pelechaty, S. M., Grotzinger, J. P., and Kaufman, A. J., 1995, Application of combined isotopic-carbon chemostratigraphy and sequence stratigraphy for basin analysis: An example from the Vendian–Cambrian interval of northeast Siberia: Geological Society of America Abstracts with Programs, v. 27, no. 6, p. A330.

Pelechaty, S. M., Grotzinger, J. P., Kashirtsev, V. A., and Zhernovsky, V. P., 1996, Chemostratigraphic and sequence stratigraphic constraints on Vendian–Cambrian basin dynamics, northeast Siberian craton: Journal of Geology, v. 104, p. 543–564.

Pokrovsky, B. G., and Missarzhevsky, V. V., 1993, Isotope correlation of Precambrian and Cambrian of the Siberian platform: Akademiya Nauk SSSR, Doklady, v. 329, p. 768–771 (in Russian).

Pokrovsky, B. G., and Venagradov, V. E., 1991, Isotopic composition of strontium, oxygen and carbon in upper Precambrian carbonates of the western area of the Anabar uplift (Kotyikan River): Akademiya Nauk SSSR, Doklady, v. 320, p. 1245–1250 (in Russian).

Read, J. F., 1983, Carbonate platform facies models: American Association of Petroleum Geologists Bulletin, v. 69, p. 1–21.

Repina, L. N., Lazarenko, N. P., and Meshkova, N. P., 1974, Lower Cambrian. Biostratigraphy and facies of Kharaulakh: Moscow, Nauka, 300 p. (in Russian).

Ripperdan, R. L., 1994, Global variations in carbon isotope composition during the latest Neoproterozoic and earliest Cambrian: Annual Reviews in Earth and Planetary Sciences, v. 22, p. 385–417.

Rodgers, J., 1991, Fold-and-thrust belts in sedimentary rocks. Part 2: Other examples, especially variants: American Journal of Science, v. 291, p. 825–886.

Sadler, P. M., 1981, Sediment accumulation rates and the completeness of stratigraphic sections: Journal of Geology, v. 89, p. 569–584.

Sadler, P. M., 1987, Sedimentation rates: Are thicker sections more complete?: Geological Society of America Abstracts with Programs, v. 19, p. 827.

Schidlowski, M., Matzigkeit, U., and Krumbein, W. E., 1984, Superheavy organic carbon from hypersaline microbial mats: Naturwissenschaften, v. 71, p. 303–308.

Schlager, W., 1981, The paradox of drowned reefs and carbonate platforms: Geological Society of America Bulletin, v. 92, p. 197–211.

Sears, S. O., and Lucia, F. J., 1980, Dolomitization of northern Michigan Niagara reefs by brine refluxion and freshwater/seawater mixing, *in* Zenger, D. H., Dunham, J. B., and Ethington, R. L., eds., Concepts and models of dolomitization: Society of Economic Paleontologists and Mineralogists Special Publication 28, p. 215–235.

Shapovalova, E. G., and Shpunt, B. R., 1982, Chapter 2: Stratigraphy, *in* Shpunt, B. R., Shapovalova, E. G., and Shamshena, E. A., eds., Late Precambrian of the northern Siberian platform: Novosibersk, Russian Academy of Science, 224 p. (in Russian).

Shenfel, V. Y., 1991, Late Precambrian of the Siberian platform: Novosibersk, Science Academy of USSR, 185 p. (in Russian).

Sheppard, S. M. F., and Schwarcz, H. P., 1970, Fractionation of carbon and oxygen isotopes and magnesium between coexisting metamorphic calcite and dolomite: Contributions to Mineralogy and Petrology, v. 26, p. 161–198.

Sokolov, B., and Fedonkin, M. A., 1984, The Vendian as the terminal system of the Precambrian: Episodes, v. 7, p. 12–19.

Tucker, M. E., 1983, Calcitic, aragonitic and mixed calcitic-aragonitic ooids from the mid-Proterozoic Belt Supergroup, Montana: Sedimentology, v. 31, p. 627–644.

Tucker, M. E., 1986, Formerly aragonitic limestones associated with tillites in the Late Proterozoic of Death Valley, California: Journal of Sedimentary Petrology, v. 56, p. 818–830.

Vail, P. R., Hardenbol, J., and Todd, R. G., 1984, Jurassic unconformities, chronostratigraphy, and sea-level changes from seismic stratigraphy and biostratigraphy, *in* Schlee, J. S., ed., Interregional unconformities and hydrocarbon accumulations: American Association of Petroleum Geologists Memoir 36, p. 129–144.

Valkov, A. K., 1987, Biostratigraphy of the Lower Cambrian of the east Siberian platform: Moscow, Moscow Science, 136 p. (in Russian).

Vidal, G., Moczydlowsky, M., and Rudavskaya, V. R., 1995, Constraints on the Early Cambrian radiation and correlation of the Tommotian and Nemakit-Daldynian regional stages of eastern Siberia: Geological Society of London Journal, v. 152, p. 499–510.

Vodanjuk, S. A., 1989, Soft-bodied metazoan remains of the Khatyspyt Formation, Olenek uplift, *in* Khomentovsky, V. V., Sovetov, Y. K., Shenfel, V. Y., Yakshen, M. C., and Moryaken, V. B., eds., Late Precambrian and early Paleozoic of Siberia: Questions of stratigraphy: Novosibersk, Russian Academy of Sciences, p. 61–74 (in Russian).

Walker, R. G., and Cant, D. J., 1984, Sandy fluvial systems, *in* Walker, R. G., ed., Facies models: Geoscience Canada, v. 1, p. 71–90.

Walter, M. R., Veevers, J. J., Calver, C. R., and Grey, K., 1995, Neoproterozoic stratigraphy of the Centralian superbasin, Australia: Precambrian Research, v. 73, p. 173–195.

Waschbusch, P. J., and Royden, L. H., 1992, Spatial and temporal evolution of foredeep basins: Lateral strength variations and inelastic yielding in continental lithosphere: Basin Research, v. 4, p. 179–196.

Zempolich, W. G., Wilkinson, B. H., and Lohmann, K. C., 1988, Diagenesis of Late Proterozoic carbonates: The Beck Spring Dolomite of eastern California: Journal of Sedimentary Petrology, v. 58, p. 656–672.

MANUSCRIPT RECEIVED BY THE SOCIETY MARCH 14, 1995
REVISED MANUSCRIPT RECEIVED OCTOBER 18, 1995
MANUSCRIPT ACCEPTED DECEMBER 21, 1995

Printed in U.S.A.